94
4/16/79

MASTER

LA. 2429

MLM-2589

Electrical Resistivity of TiH_x and $TiH_x/KClO_4$

Koto White, John W. Reed, Calvin M. Love,

Jerome E. Glaub and John A. Holy

March 16, 1979

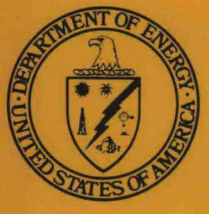

MOUND FACILITY
Miamisburg, Ohio 45342

operated by
MONSANTO RESEARCH CORPORATION
a subsidiary of Monsanto Company

for the
U. S. DEPARTMENT OF ENERGY

Contract No. DE-AC04-76-DP00053

Monsanto

PRINTED IN THE UNITED STATES OF AMERICA

Available from
National Technical Information Service
U. S. Department of Commerce
5285 Port Royal Road
Springfield, Virginia 22161
Price: Printed Copy $4.00; Microfiche $3.00

DISCLAIMER

MLM-2589
UC-45

Electrical Resistivity of TiH_x and $TiH_x/KClO_4$

Koto White, John W. Reed, Calvin M. Love, Jerome E. Glaub and John A. Holy

Issued: March 16, 1979

MOUND FACILITY
Miamisburg, Ohio 45342

operated by
MONSANTO RESEARCH CORPORATION
a subsidiary of Monsanto Company

for the
U. S. DEPARTMENT OF ENERGY

Contract No DE-AC04-76-DP00053

Contents

Published by Information Services
William C. Shumay, Jr., Editor

Abstract

Various factors affecting the electrical resistivity of the pyrotechnic pressed powder $TiH_x/KClO_4$, which is sensitive to hot wire ignition yet quite spark insensitive, were evaluated. The electrical resistivity of the TiH_x and $TiH_x/KClO_4$ were correlated with their pressing pressure, stoichiometry, powder surface area, and temperature (from below liquid nitrogen temperature to 500 K). Data show resistivity increasing with x and surface area, and decreasing non-linearly with pressing pressure. It was concluded that temperature coefficient of resistivity depends upon powder surface features. In addition, it was found that electrostatic discharge lowers TiH_x and $TiH_x/KClO_4$ pellet resistivity and that the effect is larger for pellets with higher initial resistivity.

Introduction

Electrical properties of pyrotechnic compositions are important because these properties affect ignition behavior. In actuators and ignitors that make use of a bridgewire, sufficient electrical conductivity on the part of the pyrotechnic material in contact can allow the establishment of a parallel electrical path between the bridgewire posts. With the low energy delivered to this type of device, a parallel-path condition can cause insufficient bridgewire heating. The objective of this project was to determine and evaluate factors that affect the electrical resistivity of pyrotechnic material. Since a pressed-powder mixture of titanium subhydride (TiH_x) and potassium perchlorate ($KClO_4$) is used in certain pyrotechnic valve actuators, these two materials, individually and blended, were studied.

Four-probe resistivity measurement

All resistivity measurements were made using the four-probe technique illustrated in Figure 1. An electrical current is carried through the two outer probes, which sets up an electric field in the sample (in the figure, the electric field lines are solid and the equipotential lines are broken), and the two inner probes measure the potential difference between point B and point C. These inner probes draw no current because of the high input impedance ($10^9\Omega$) voltmeter in the circuit. Thus, unwanted voltage drop (IR drop) at point B and point C caused by contact resistance between probes and the sample is eliminated from the potential measurements. Since these contact resistances are very sensitive to pressure and to surface condition (such as oxidation of either surface), error with the conventional two-electrode technique (in which the potential-measuring contact passes a current) can be quite large. With a four-point probe of equal spacing, ρ (resistivity, ohm-

centimeters) of sample can be calculated [1] [2] from the measured quantities: V (potential difference between point B and point C in Figure 1, volts), I (current, amperes) and S (electrode spacing, centimeters). The equation used is:

$$\rho = 2\pi S \cdot \frac{V}{I}$$

Resistivity as a function of pellet characteristics

All resistivity measurements in this section were made using a spring-loaded four-point probe of equal probe spacing (0.025 in.), manufactured by Alessi Industries. For each sample pellet, resistivities of four different locations on each pellet side were averaged to obtain the average pellet resistivity.

Pressed TiH_x pellets

In order to investigate the factors affecting the resistivity of pressed TiH_x pellets at room temperature, 10 different batches of TiH_x powder were selected from the stoichiometry groups of x=1.9, 1.5, 0.65, and 0.19. Each group included a batch with high surface area and a batch with low surface area. Each batch of material was pressed into several pellets with pressing pressures varying from 10 to 160 kpsi. The results as a function of pellet density are shown in Figure 2.

Our findings were:

(1) When resistivities were compared within a similar stoichiometric group, higher surface area material generally showed a higher resistivity.

(2) A resistivity versus stoichiometry relationship was seen for a group of high surface area materials, with a high stoichiometry apparently resulting in a high resistivity. The difference in resistivity between x=0.19 and x=1.9 is about two orders of magnitude. (See Figure 3)

(3) The difference in resistivity between batches was larger at the lower pellet density.

The resistivity data of Andrievskii [3] on hydrided titanium rod shows a weaker stoichiometric dependence. As shown in Figure 4, Andrievskii observed the change in resistivity of about a factor of two, compared to our observations of two orders of magnitude with pressed pellets. A possible explanation for this difference is that the individual TiH_x powder particles are coated with titanium oxide.

As shown in a hypothetical picture of powder particles (Figure 5), overall resistivity of the sample has three components. One component is the resistivity of the titanium hydride particle core, which is on the order of $\sim 10^{-4}\ \Omega\cdot cm$. A second component is the resistance from the titanium oxide layer, which depends upon the layer's composition and defect structure as well as its thickness, and may be $10^{-2}\ \Omega\cdot cm$ to $10^{11}\ \Omega\cdot cm$. A third component is the contact resistance between adjacent powder particles, which is likely to be dependent on the pressing pressure, surface area, and particle size distribution. It's expected to be much greater than $10^{-4}\ \Omega\cdot cm$. Since the first component is most likely much smaller than the others,

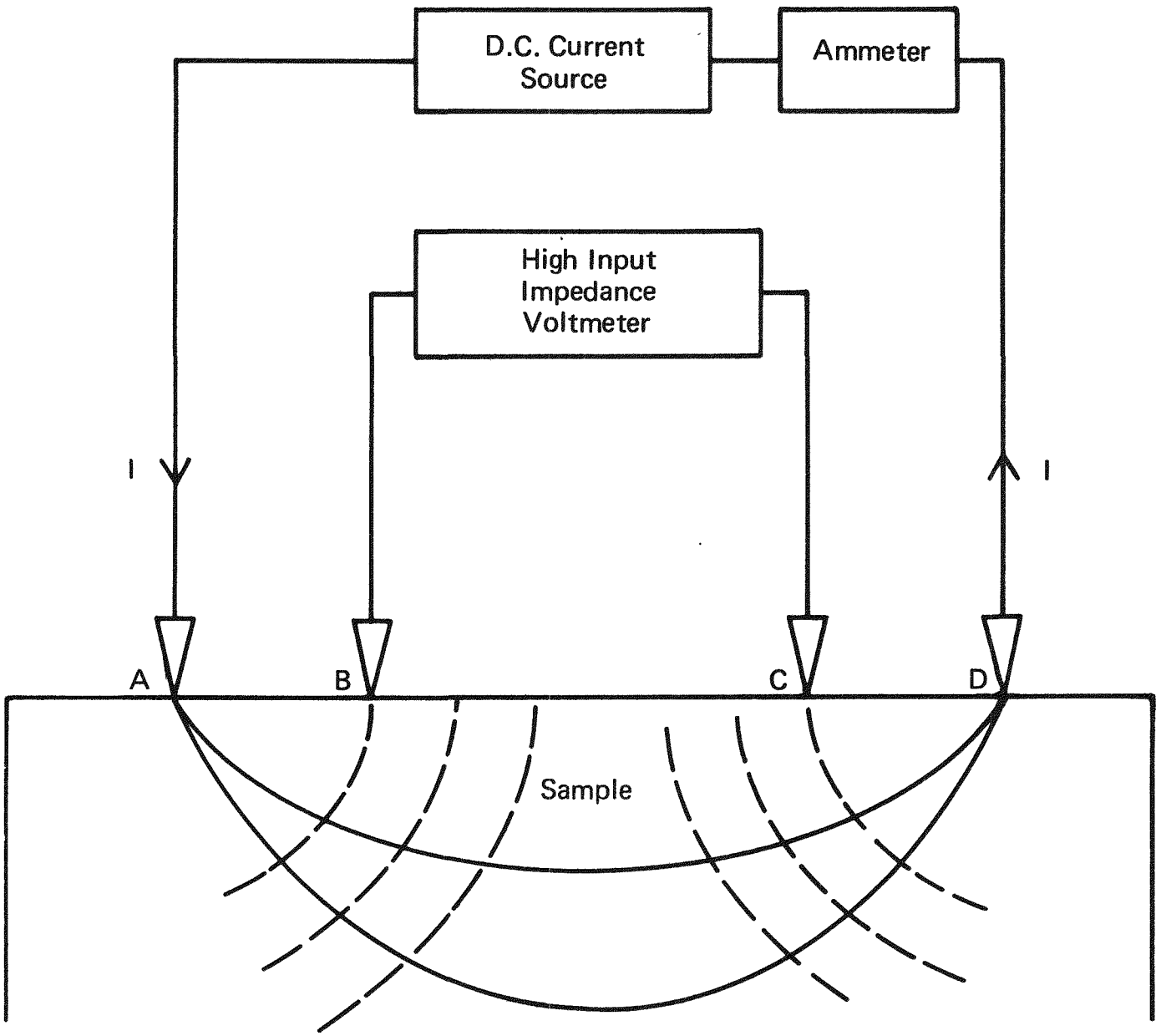

FIGURE 1 - Four-point probe for resistivity measurements.

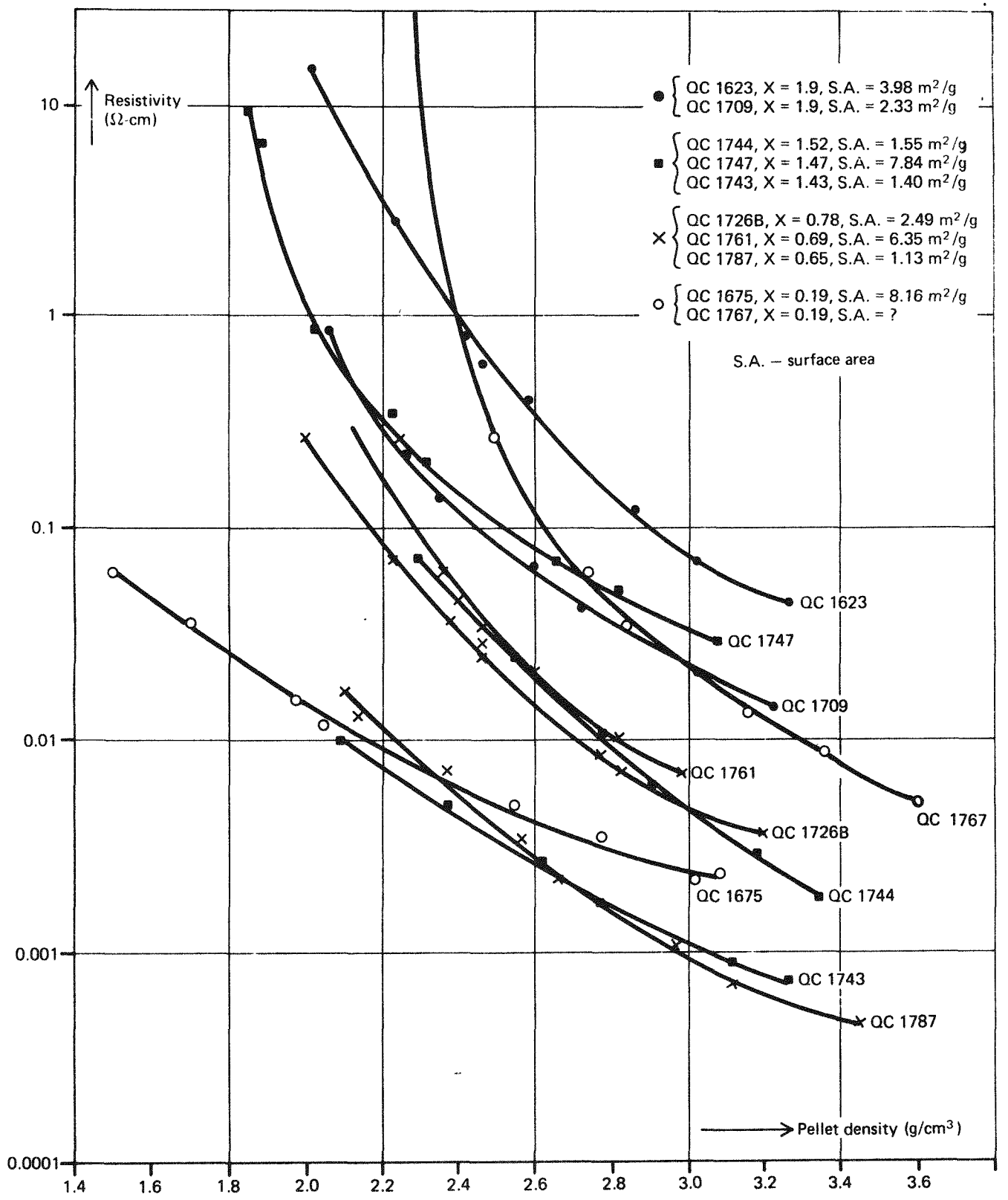

FIGURE 2 - Resistivity of TiH_x pressed pellets.

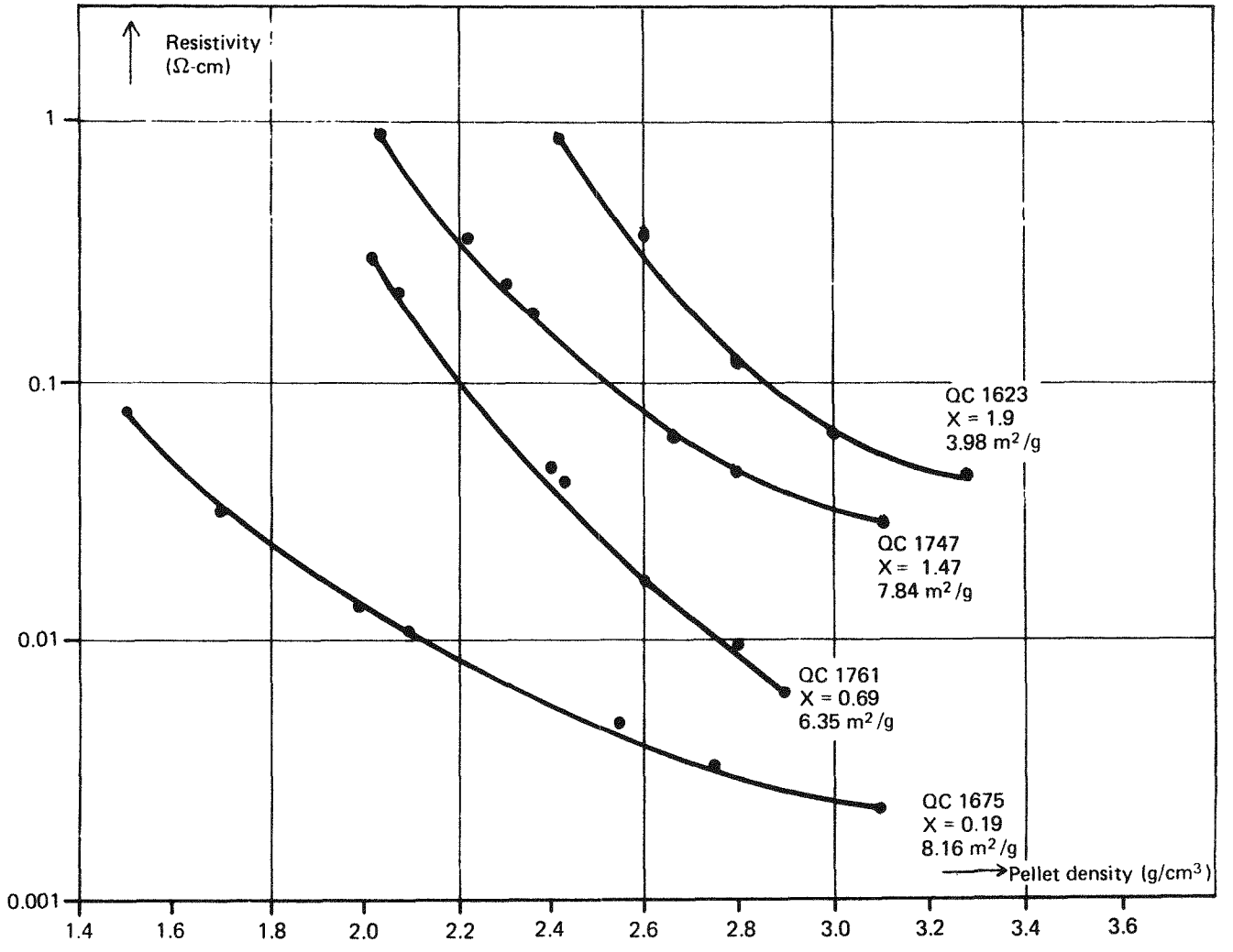

FIGURE 3 - Resistivity of high surface area TiH_x pressed pellets.

the resistivity variation we observed between different batches and different pressing pressures must be caused by the second and/or third components.

Pressed $TiH_x/KClO_4$ pellets

Several batches of $TiH_x/KClO_4$ (33/67 wt %) blends with various TiH_x stoichiometries were pressed into pellets using pressures of 10 and 20 kpsi. Results of resistivity measurements are shown in Figure 6. It can be seen that when TiH_x is mixed with $KClO_4$, hydride stoichiometry becomes the dominating factor. A difference in resistivity of six orders of magnitude was observed between materials with x=0.19 and x=1.9. This can be compared to two orders of magnitude difference observed for TiH_x without $KClO_4$. These results indicate that titanium subhydrides of different stoichiometries are interacting with their environment to considerably

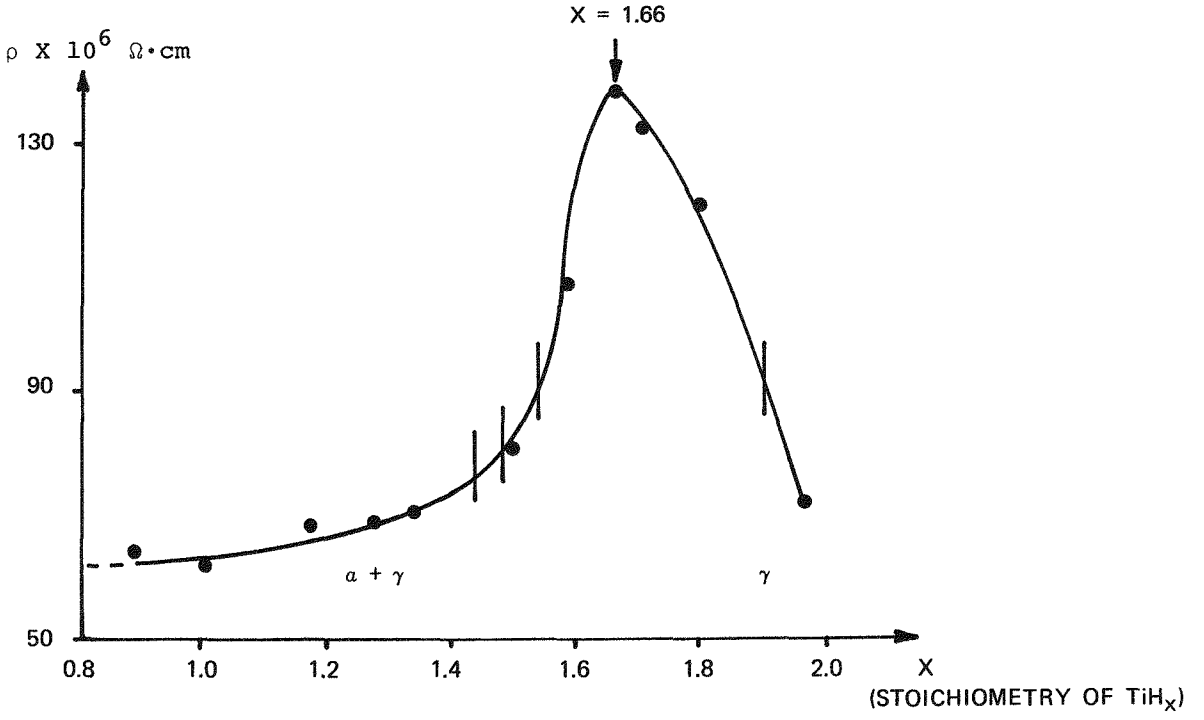

FIGURE 4 - a + y phase resistivity data according to Andrievskii [3]
(sample is in the form of hydrided Ti rod)

different extents in the presence of $KClO_4$. It is possible that the variation is due to the difference between rutile and defective (or mixed phase) titanium oxide on the particle surface. Table I shows the resistivity of titanium oxide as reported in literature. [4] Departure from $TiO_{2.000}$ stoichiometry is seen to drastically reduce titanium oxide resistivity.

Resistivity as a function of temperature

A cryostat system capable of attaining from 3 to 500 K was constructed to investigate the effect of temperature on resistivity. The cryostat (Oxford Instrument Model CF 100) was cooled by a controlled, continuous flow of liquid helium delivered through a transfer tube from a 60-liter storage vessel. A 39 Ω internal heater on the heat exchange block and a temperature controller (Oxford Instrument Model DTC2) were used along with helium flow to maintain any desired temperature. Two thermocouples were located inside the cryostat. One, on the heat exchange block, monitored the heater output; the other was used for sample temperature measurement and for indication of thermal equilibrium. Cold exhaust helium gas returning from the cryostat insulated the transfer tube, as did an evacuated space in the outer jacket. Two vacuum spaces separated by a radiation shield insulated the cryostat. The initial checkout of the system was accomplished using a piece of titanium metal as a standard sample.

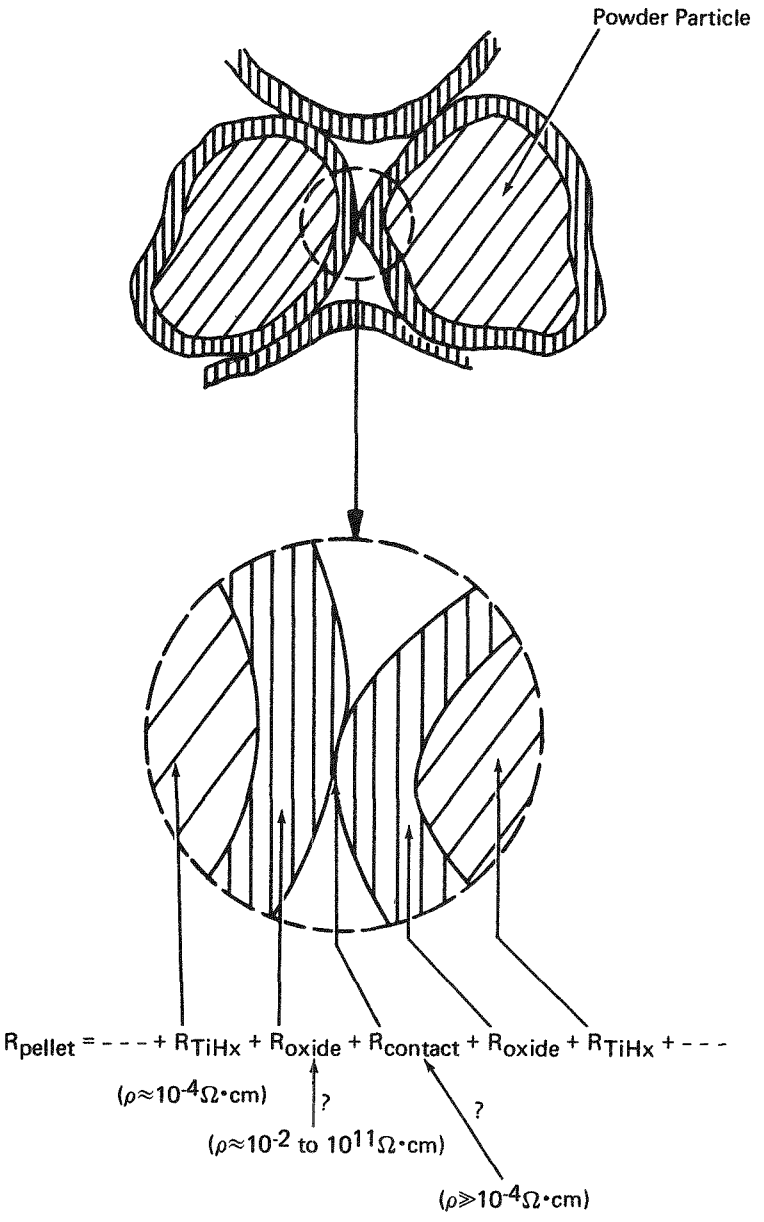

FIGURE 5 - A hypothetical picture of powder particles.

The probe spacer was made of reinforced phenolic to better withstand the thermocycle.

A schematic diagram of the experimental setup is shown in Figure 7.

Pressed TiH_x pellets

Fourteen samples of pressed TiH_x pellets were examined in this study. A thermocycle consisted of: (1) cooling to 70 K, (2) heating to 460 K (sometimes up to 500 K), and (3) cooling back to the room temperature. The heating and cooling rates were held close to 10°C/min, and

Table 1 - TiO_x Resistivity

x	2.0000	1.9995	1.995	1.75
ρ	10^{10}	10	1.25	10^{-2} Ω cm

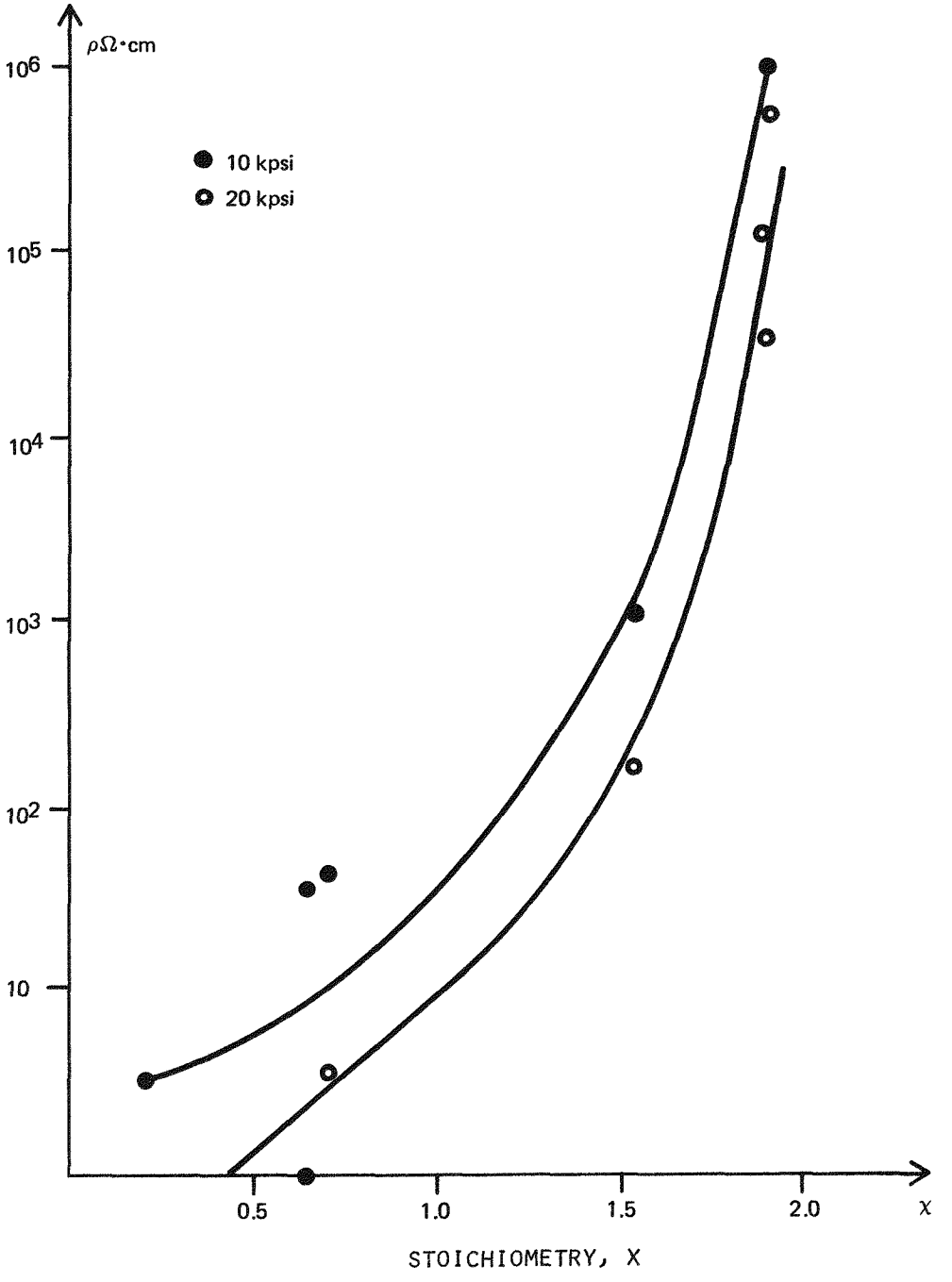

FIGURE 6 - Resistivity of $TiH_x/KClO_4$ pressed pellets.

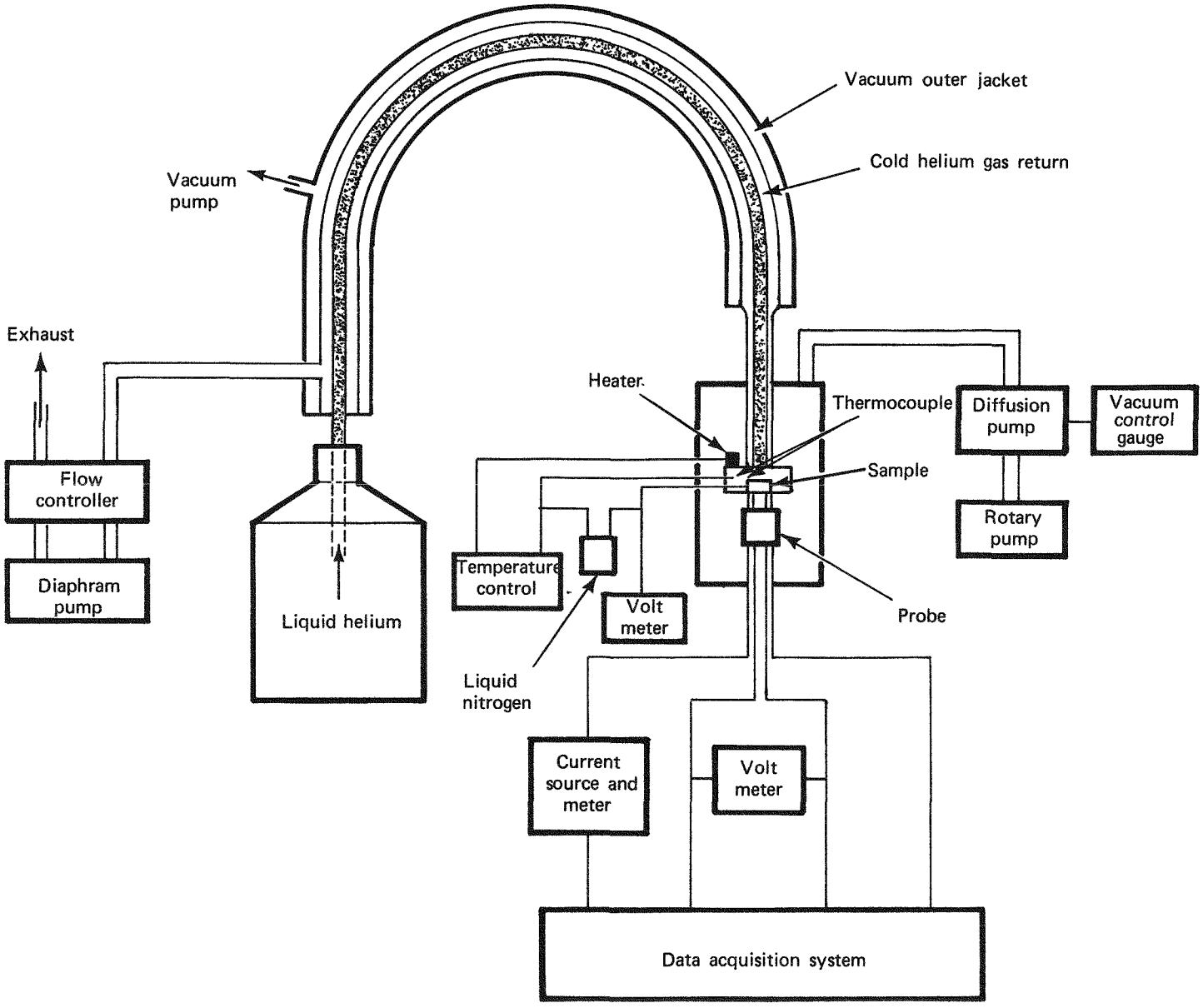

FIGURE 7 - Schematic diagram for temperature experiment.

the samples were soaked at each temperature for 10 min before the measurements were taken. Any residual voltage output (that is, voltage output when no current is delivered to the sample) was probably caused by thermal EMF's of various connections in the measuring circuit and was subtracted from each reading.

All resistivity data (ρ) obtained as a function of temperature (T) were normalized by dividing by the room temperature resistivity value (ρ_o). Therefore, the slope of this $\frac{\rho}{\rho_o}$ vs. T curve is a visual indication of the temperature coefficient of resistivity (α), that is,

$$\alpha = \frac{1}{\rho_o} \frac{\partial \rho}{\partial T}$$

This allows comparison of various sets of data in different resistivity ranges and also permits visualization of percentage changes in resistivity during each thermocycle. The resistivity value at room temperature before going through the thermocycle was taken to be 100%.

In these experiments, the observed change in resistivity during the thermocycle is most likely caused by resistivity changes of powder surface coatings and changes in contact resistance between adjacent powder particles.

The group of $TiH_{1.9}$ samples showed large negative temperature coefficients (Figures 8-12), which indicates that the material probably has a semiconductor-like oxide coating. The high surface area samples (Figures 8 and 9) showed much steeper slopes compared to the low surface area samples (Figures 10-12). When the data are compared as a function of pressing pressure, the pellets pressed at lower pressures show slightly larger variations over identical temperature intervals. One can see that the powder contraction and expansion contributes to a negative temperature coefficient. This is an indication that the $TiH_{1.9}$ powder particles contract and expand noticeably with temperature and the larger surface area enhances this effect on resistivity.

For $TiH_{0.65}$ and $TiH_{0.19}$ samples, variation in slope from different pressing pressures was very slight. The samples with high surface area showed a slightly negative temperature coefficient (Figures 13, 14, 18 and 19); whereas the ones with lower surface area showed a slightly positive temperature coefficient (Figures 15, 16, 17, 20 and 21) at below room temperature. This might indicate that the surface of $TiH_{0.65}$ and $TiH_{0.19}$ is dominated by an oxide with a slightly positive temperature coefficient that is partially cancelled by the negativeness in slope due to particle expansion and contraction.

As for the region above $\sim$400 K, all samples examined showed a decrease in resistivity upon heating. Also, once the samples were heated to above $\sim$400 K, the cooling curve did not coincide with the heating curve; and it was observed that the magnitude of permanent reduction in sample resistivity upon heating depends on maximum temperature exposure. This suggests some irreversible change in material occurs, such as off-gassing of surface hydrogen or moisture, a break in the surface coating, or annealing of the surface coating.

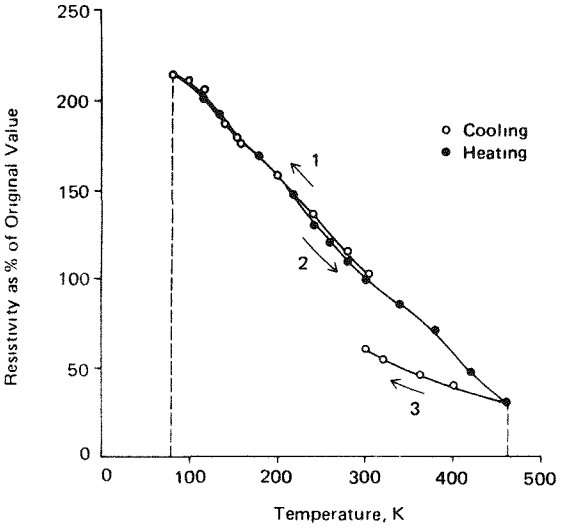

FIGURE 8 - $TiH_{1.9}$, HIGH S.A. 100 kpsi

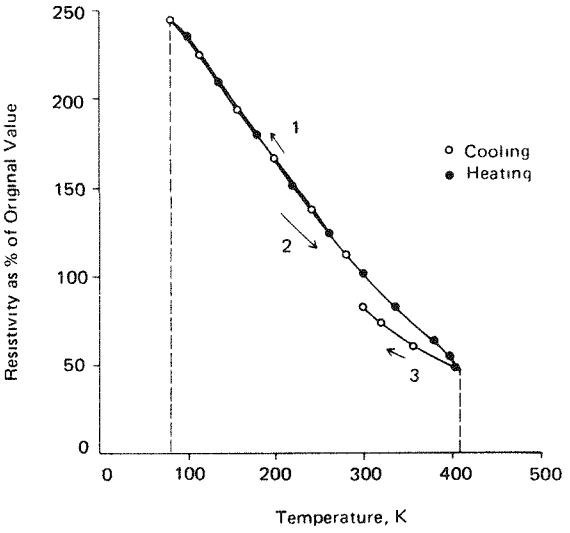

FIGURE 9 - $TiH_{1.9}$, HIGH S.A. 70 kpsi

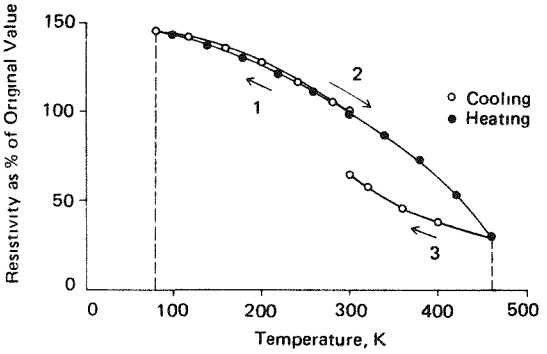

FIGURE 10 - $TiH_{1.9}$, LOW S.A. 100 kpsi

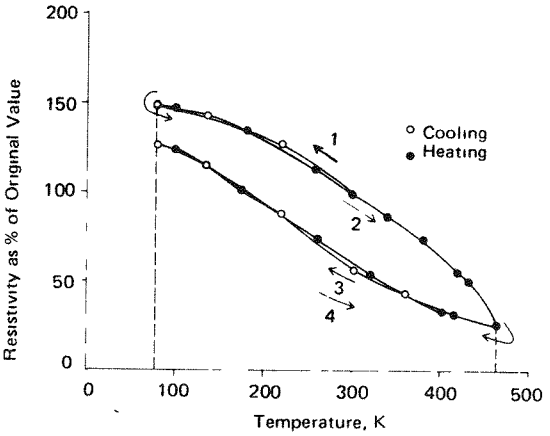

FIGURE 11 - $TiH_{1.9}$, LOW S.A. 70 kpsi

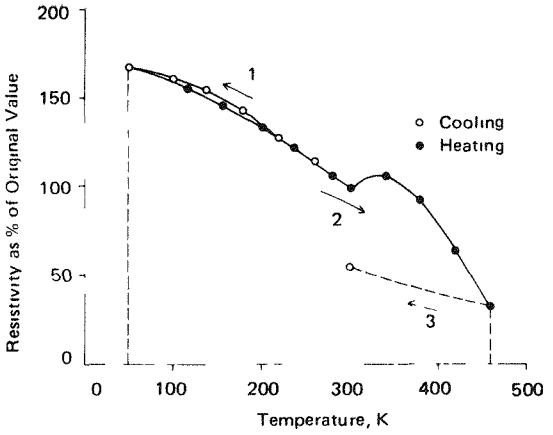

FIGURE 12 - $TiH_{1.9}$, LOW S.A. 40 kpsi

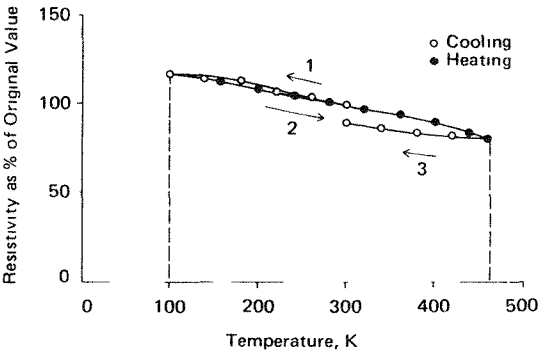

FIGURE 13 - $TiH_{0.65}$, HIGH S.A. 100 kpsi

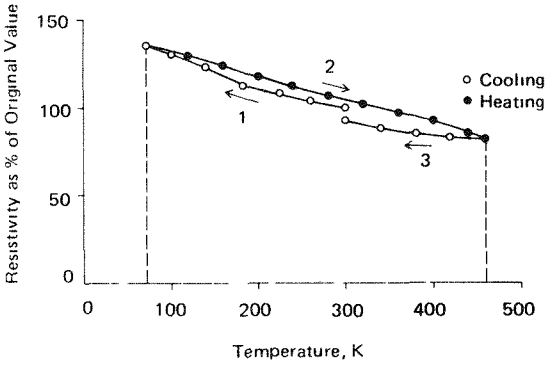

FIGURE 14 - $TiH_{0.65}$, HIGH S.A. 70 kpsi

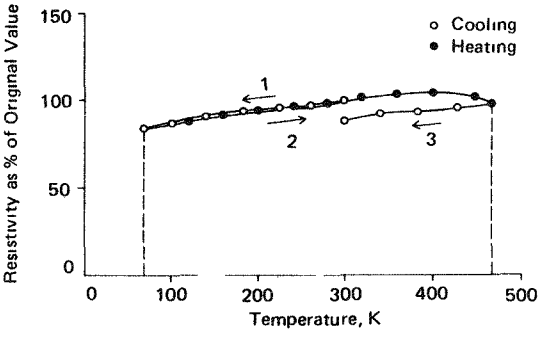

FIGURE 15 - $TiH_{0.65}$, LOW S.A. 70 kpsi

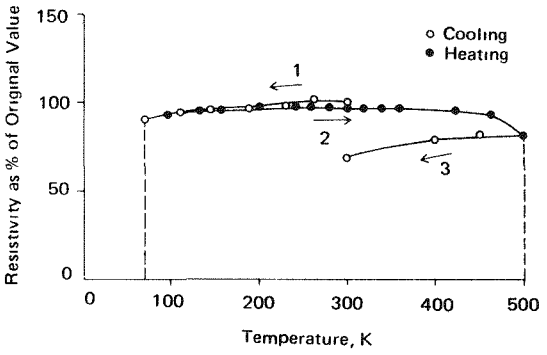

FIGURE 16 - $TiH_{0.65}$, LOW S.A. 40 kpsi

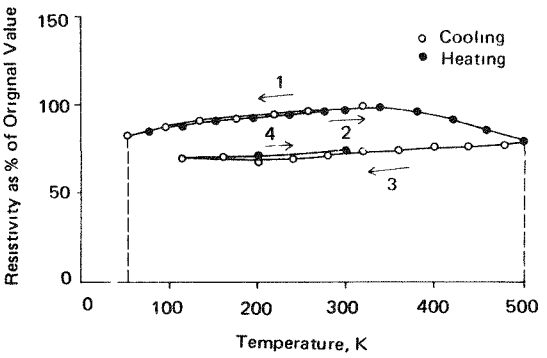

FIGURE 17 - $TiH_{0.65}$, LOW S.A. 30 kpsi

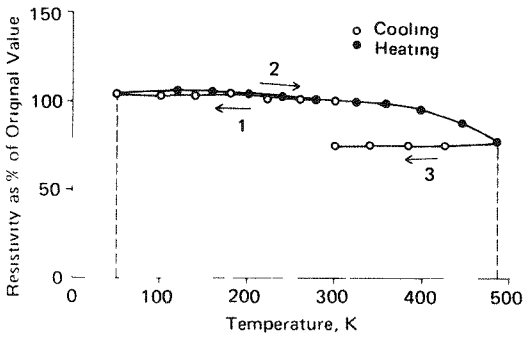

FIGURE 18 - $TiH_{0.19}$, HIGH S.A. 100 kpsi

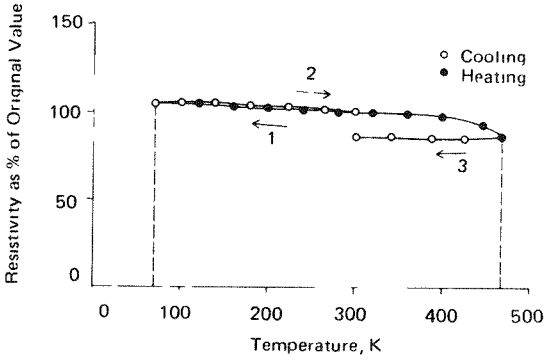

FIGURE 19 - $TiH_{0.19}$, HIGH S.A. 40 kpsi

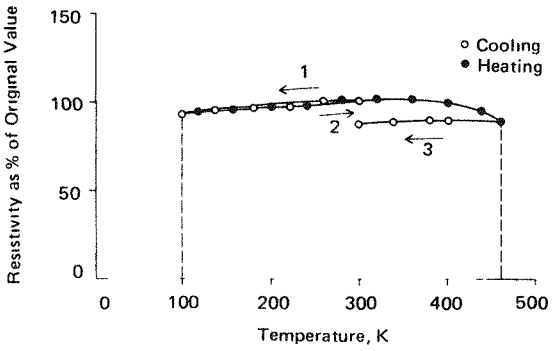

FIGURE 20 - $TiH_{0.19}$, UNKNOWN S.A. 100 kpsk

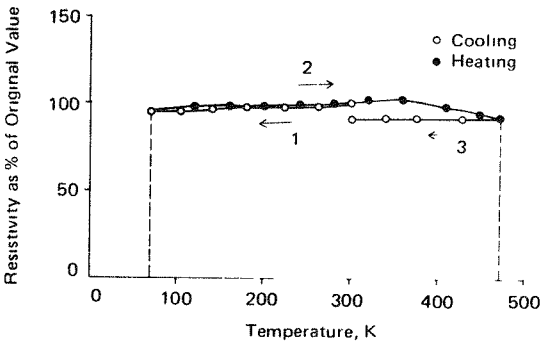

FIGURE 21 - $TiH_{0.19}$, UNKNOWN S.A. 40 kpsi

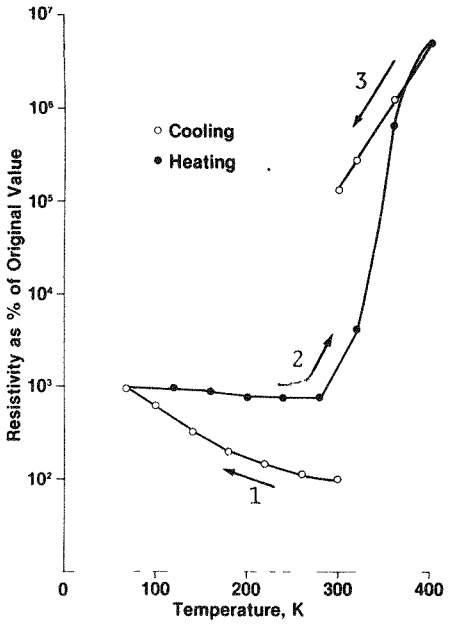

FIGURE 22 - PE3087($TiH_{1.11}$/$KClO_4$)
20 kpsi, #1

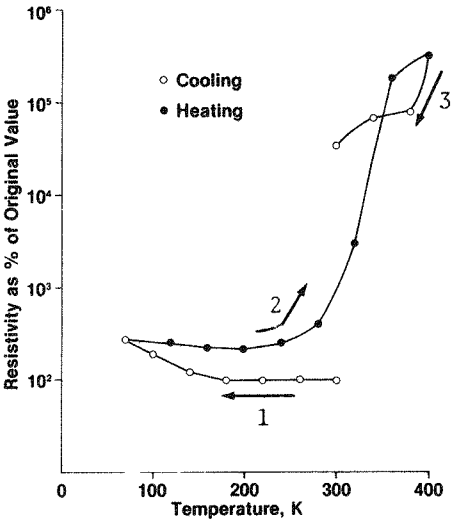

FIGURE 23 - PO3087($TiH_{1.11}$/$KClO_4$)
20 kpsi, #2

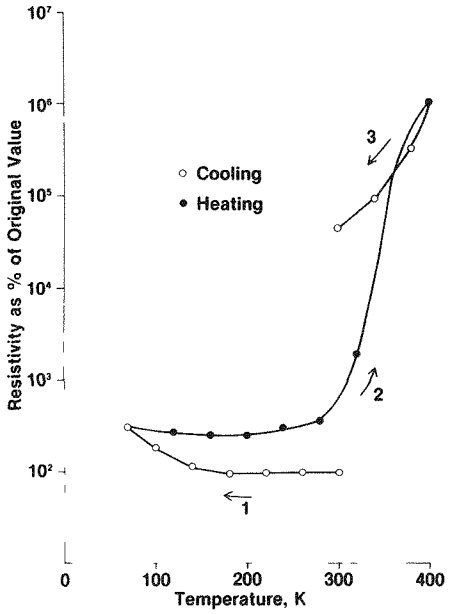

FIGURE 24 - P03087 ($TiH_{1.11}/KClO_4$)
20 kpsi, #3

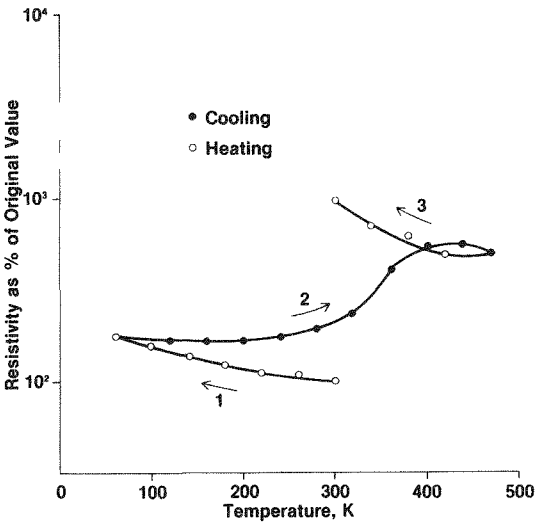

FIGURE 25 - PA8 ($TiH_{0.65}/KClO_4$)
20 kpsi, #1

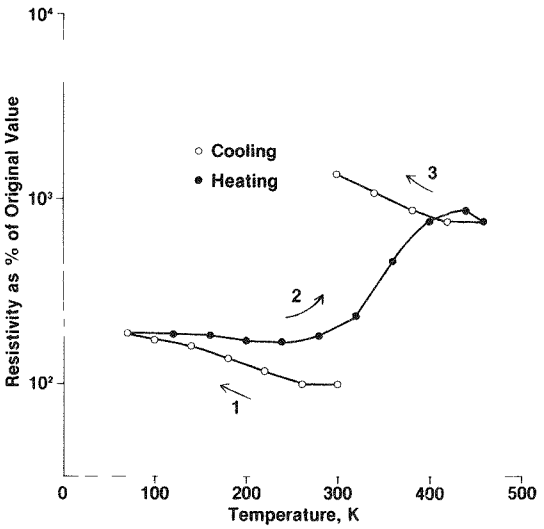

FIGURE 26 - PA8 ($TiH_{0.65}/KClO_4$)
20 kpsi, #2

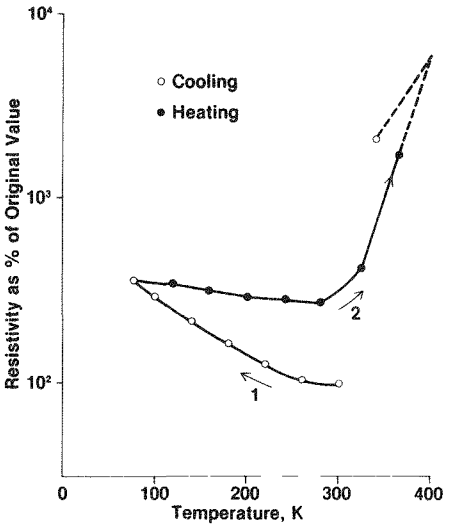

FIGURE 27 - P03088 ($TiH_{0.65}/KClO_4$)
20 kpsi

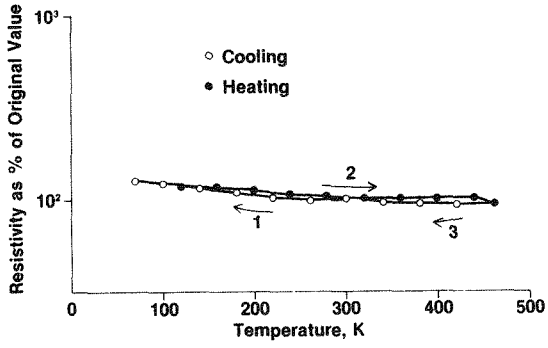

FIGURE 28 - PB7 ($TiH_{0.19}/KClO_4$)
20 kpsi, #1

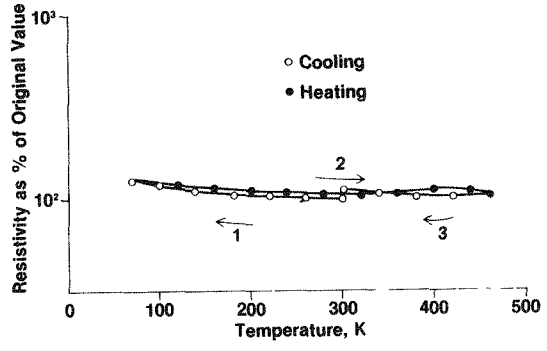

FIGURE 29 - PB7 ($TiH_{0.19}/KClO_4$)
20 kpsi, #2

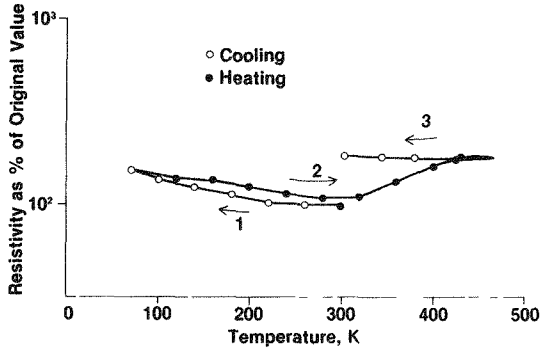

FIGURE 30 - P02040 ($TiH_{0.19}/KClO_4$) 20 kpsi

Some of the samples were analyzed for hydrogen content after the thermocycle. No change in bulk hydrogen content was detected.

An attempt was made to see if the decrease in resistivity upon heating above ∿400 K was due to loss of moisture. Figuring to suppress the possible offgassing of water from the samples in the 10^{-5} torr vacuum, some above room temperature experiments were conducted in a static helium atmosphere and some experiments were performed in air with no significant difference in results.

Pressed $TiH_x/KClO_4$ pellets

Five batches of blend materials were selected from three stoichiometric groups of TiH_x (x=0.19, 0.65, and 1.11). Pressing pressure of the pellets was 20 kpsi.

As can be seen in Figures 22-30, resistivity generally increased when the temperature was lowered, which was probably caused by powder contraction. Even after the sample was rewarmed, the resistivity remained higher. This was possibly caused by permanent shifting of the powder due to differences in thermal expansion coefficients between TiH_x, the surface coating, and $KClO_4$. This effect was the largest for $TiH_{1.11}/KClO_4$ and negligible for $TiH_{0.19}/KClO_4$ as can be seen by comparing Figures 22-24 with Figures 28-30. The resistivity of $TiH_{1.11}/KClO_4$ increased very rapidly (by six orders of magnitude) when heated, while $TiH_{0.19}/KClO_4$ showed very little change. This might be due to factors dependent on the hydride stoichiometry at each temperature range.

Similar pellets behaved more or less in the same way, as can be seen by comparing Figures 22-24 (the sample for Figure 22 being pressed 2 years earlier), Figures 25 and 26, and Figures 28 and 29. For $TiH_{1.11}/KClO_4$, reproducibility of data seems to depend on the soaking time at each temperature.

Effect of electrostatic discharge on pellet resistivity

All measurements shown here were made using an Alessi Industries eight-probe station. The probe spacing was adjusted to S=0.020 in.

The electrostatic pulse was generated by discharging a 600 PF capacitor through a 500 Ω resistor to simulate a human body electrostatic discharge. The capacitor was charged at 5 kV for all tests. The discharge path was either between four probes and a fifth probe on the same face of the pellet, or between four probes and the entire opposite face of the pellet. Resistivity was measured both before and after the sample received an electrostatic pulse.

For both TiH_x and $TiH_x/KClO_4$ (Figures 31 and 32) the electrostatic pulse had no effect when the resistivity of the pellets was lower than 1 Ω·cm. The pellets with higher resistivity, however, were all affected by the pulses. For very high resistivity pellets, the resistivity decreased by orders of magnitude after being pulsed. A possible explanation for this behavior can be found in the way the pellets were pulsed. Since we had a 500 Ω resistor in series with the pellet, and the total power (Q_o) available in the capacitor is a fixed value

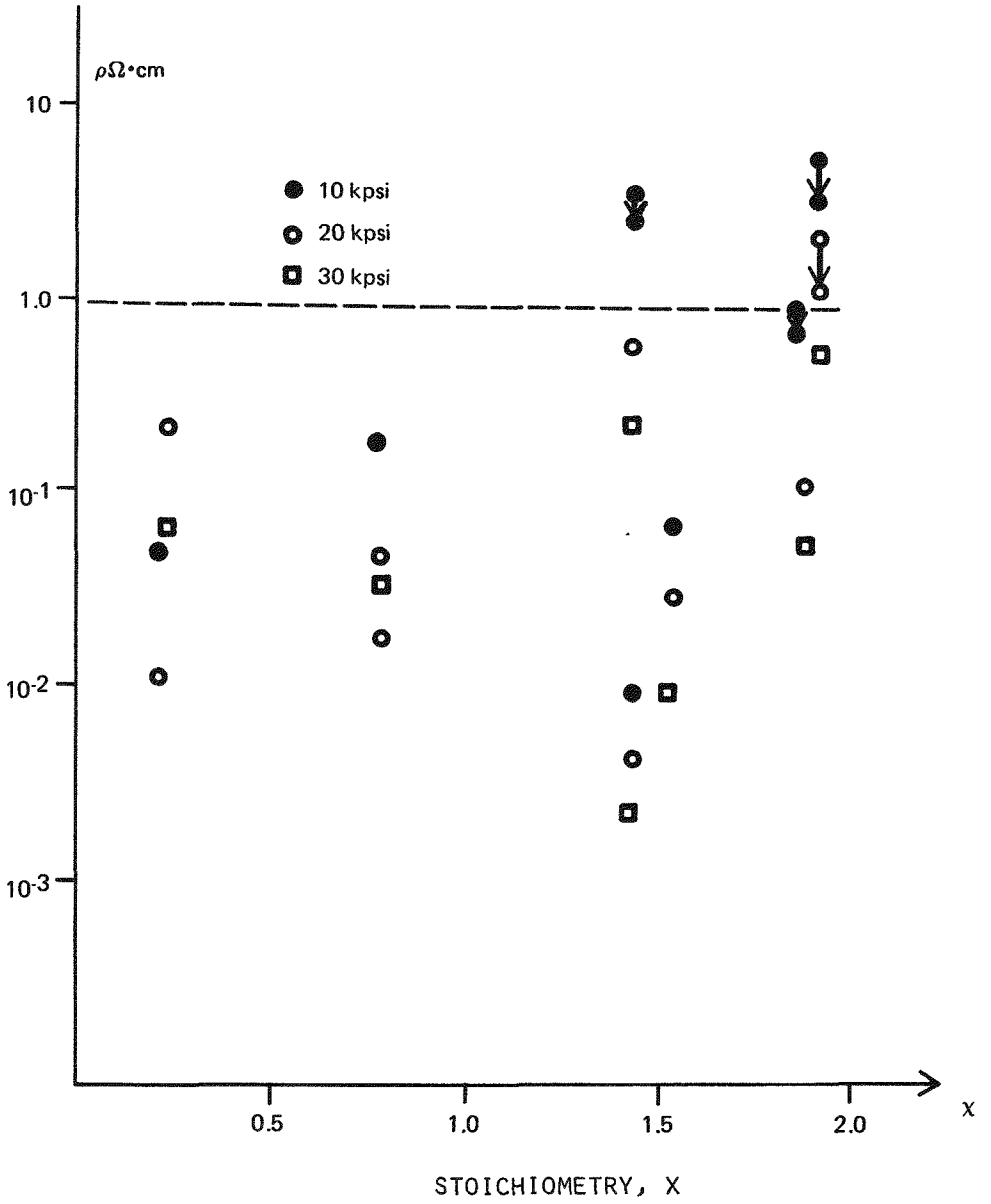

FIGURE 31 - 5 kV Electrostatic Test on $TiH_x/KClO_4$.

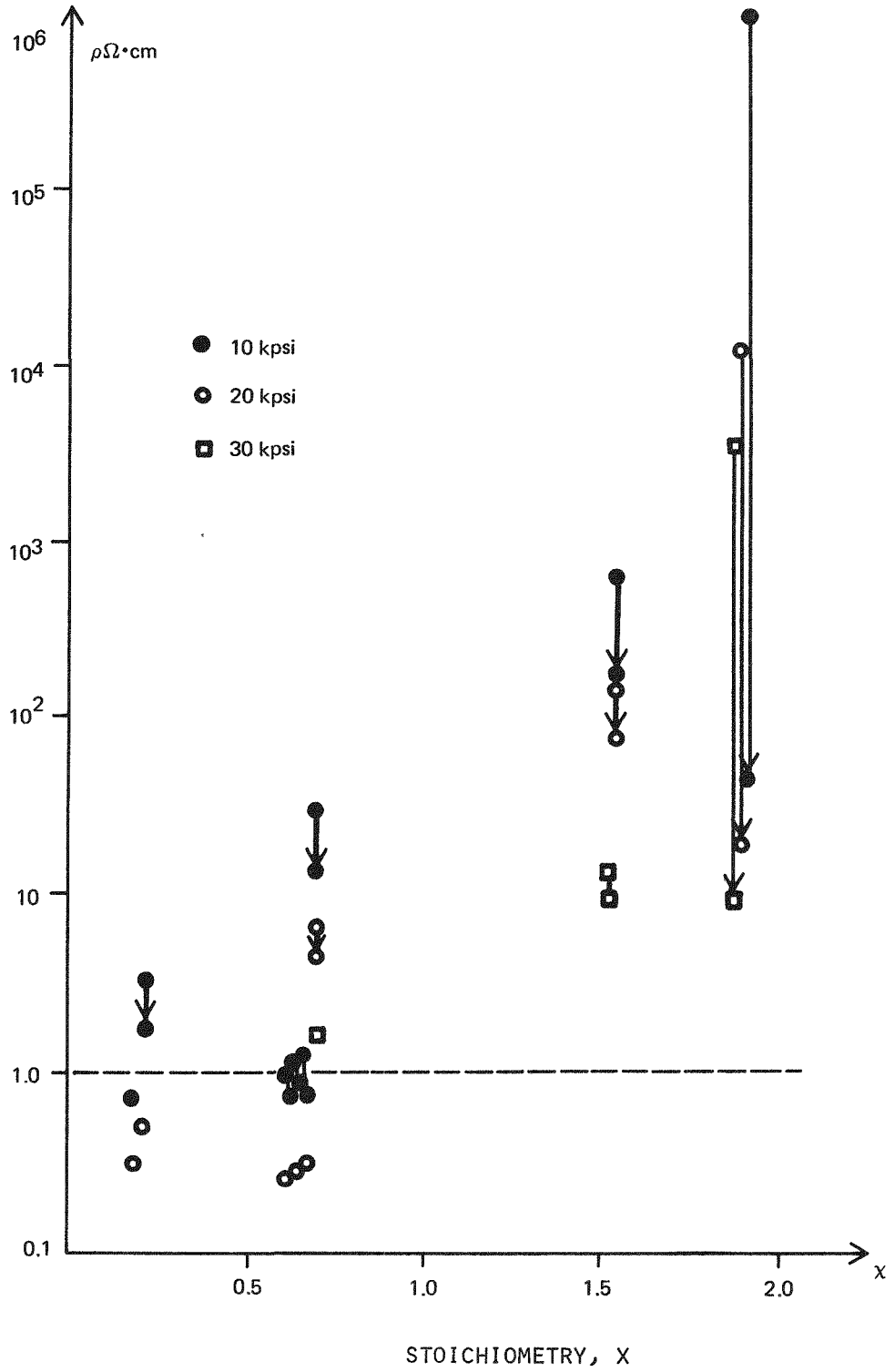

FIGURE 32 - 5 kV Electrostatic Test on $TiH_x/KClO_4$.

in this experiment, the power actually delivered to the pellet (Q_{pellet}) is described as:

$$Q_{pellet} = \frac{R}{R + 500} \cdot Q_o$$

where R is the resistance of the discharge path through the pellet. Thus, for the pellets with approximately megaohm range resistance, almost all the power is dissipated in the pellet; whereas for the low resistivity pellets, only a small percentage of the total power is dissipated in the pellet.

Overall reduction in resistivity might be caused by fractures in the surface oxide coating, or by further introduction of defects into the oxide structure when subjected to the pulse. Defective TiO_2 is known to have a lower resistivity than that of rutile TiO_2.

For all the pellets examined, the current flow through the outer two probes (A and D in Figure 1) increased after pulsing even for low resistivity samples whose resistivity was not affected by the pulse. This may be a consequence of the probes being pushed down into the sample when subjected to pulses. (See the Appendix for details.)

Summary and conclusion

In this series of studies, we have determined the resistivity variation of pressed TiH_x and $TiH_x/KClO_4$ pellets as functions of pellet density (or pressing pressure), TiH_x stoichiometry, TiH_x powder surface area, and temperature. In addition, we studied the effects of electrostatic discharge on sample resistivity.

Resistivity of titanium hydride particle cores plays an insignificant role in overall pellet resistivity. The most probable explanation for the resistivity variations observed among different batches of materials and different pressing pressures is that the powder particles are coated with an oxide layer of varying composition, defect (mixed phase) structure, and thickness.

Stoichiometry of TiH_x is the main factor determining the resistivity of $TiH_x/KClO_4$ blend material. High stoichiometric TiH_x seems to interact with its environment more, especially in the presence of $KClO_4$.

When pressed $TiH_x/KClO_4$ pellets were heated above room temperature, increases in resistivity were very rapid (by six orders of magnitude) for $TiH_{1.11}/KClO_4$ and very little for $TiH_{0.19}/KClO_4$. When pressed TiH_x pellets were cooled below room temperature, the pellet resistivity went up because of powder contraction; but the resistivity of the oxide coating may go up or down depending on the type of oxide dominating. So, the overall temperature response of the samples is either cancellation or enhancement of these two effects. High surface area materials, when contracted by cooling, appear to contribute more to an increase in resistivity. For $TiH_{1.9}$ the dominating surface oxide seems to have a negative temperature coefficient which is, in general, a characteristic of semiconductors. For $TiH_{0.65}$ and $TiH_{0.19}$, this semiconductor-like behavior disappears.

Electrostatic discharge affects the higher resistivity material more, partly because the power delivered to the sample pellet depends on the resistance of the discharge path in the pellet. The electrical discharge seems to either break the surface oxide coating or introduce further defects into the oxide structure to reduce the resistivity.

As a general conclusion, resistivity measurements on pressed pellets indirectly show the powder surface characteristics. Some experimenters have purposely used pressed powder samples to see an enhanced effect of surface on resistivity. [5] But in our case, it is impossible to deduce the surface characteristics from these data alone or to confidently understand the physical and chemical changes taking place. Perhaps in the future, it will be possible to correlate these data with some other more direct surface analysis information.

References

1. Valdes, L. B., "Effect of Electrode Spacing on the Equivalent Base Resistance of Point-Contact Transistors", Proc. I.R.E., 40, 1429-34 (1952)
2. Valdes, L. B. "Resistivity Measurements on Germanium for Transistors", Proc. I.R.E., 40, 420-26 (1954)
3. Andrievskii, R. A., "Electrical, Magnetic and Galvanomagnetic Properties of Titanium, Hafnium and Niobium Hydrides", Russian J. Inorganic Chem., 17:4, 477-82 (1972)
4. Suchet, J. P., Crystal Chemistry and Semiconductors in Transition Metal Binary Compounds, Academic Press, N.Y., 1971.
5. Morrison, S. R., "Measurement of Surface State Energy Level of One-Equivalent Adsorbates on ZnO", Surface Science, 27, 586-604 (1971)

Appendix

The current (I) flowing through the sample can be described as:

$$I = \frac{V_o}{R + R_{contact}}$$

where

$$R = \frac{\rho}{2\pi}\left(\frac{1}{r_o} - \frac{2}{L}\right)$$

and where V_o is the voltage output of current source, $R_{contact}$ is the contact resistance between probes A, D, (Figure 1) and the sample. R is the resistance of the sample, ρ is the resistivity of the sample, r_o is the radius of the probe tip actually buried in the sample and L is the distance between point A and point D. R can be derived from calculating the power dissipated in the sample:

$$RI^2 = \iiint \rho J^2 \, d\phi \sin\theta d\theta r^2 dr$$

Since at any point in the sample, current density, $J = I/2\pi r^2$, the above equation reduces to:

$$RI^2 = \frac{\rho I^2}{2\pi} \cdot -\left[\frac{-1}{r}\right]_{r_o}^{\frac{L}{2}} = \frac{\rho I^2}{2\pi}\left(\frac{1}{r_o} - \frac{2}{L}\right)$$

Besides the reduction in resistivity, two factors exist which lead to the overall decrease in current (I). One is the reduction in contact resistance $R_{contact}$; the other is the increase in the probe tip radius (r_o) actually in contact with the sample. Since the probe tip has a conical shape, r_o increases when the probe is pushed down into the sample.

Distribution

EXTERNAL

TIC, UC-45
R. K. Flitcraft, Monsanto Research Corporation
H. N Hill, DOE/Dayton Area Office
T. W. Listerman, Wright State University
W. E. Moddeman, University of Dayton
R. N. Rogers, Los Alamos Scientific Laboratory
N. A. Schneider, Jr., Lawrence Livermore Laboratory
R. E. Taylor, Purdue University

Sandia Laboratories Albuquerque

D. H. Anderson
J. R. Craig
J. C. Crawford
R. A. Damerow
R. J. Eagan
A. K. Jacobson
R. G. Jungst
J. E. Kennedy
E. A. Kjeldgaard
W. B. Leslie
M. L. Lieberman
T. M. Massis
W. G. Perkins
R. K. Quinn
H. J. Saxton
B. R. Steele
F. J. Villa
R. E. Whan

Sandia Laboratories Livermore

M. R. Birnbaum
D. E. Gregson

INTERNAL

H. F. Anderson
R. C. Bowman, Jr.
R. T. Braun
J. R. Brinkman
R. S. Carlson
W. T. Cave
C. H. H. Chong
T. S. Chou
L. W. Collins
R. T. DeSando
R. A. Fischbein
V. M. Franchetti
C. S. Friedman
J. E. Glaub
L. D. Haws
D. L. Hobrock
J. A. Holy
C. W. Huntington
R. R. Jaeger
P. L. Johnson
C. M. Love
J. R. McClain
G. D. Miller
J. H. Mohler
A. C. Munger
R. L. Parks
K. D. Phipps
J. W. Reed
M. C. Rey
W. C. Shumay
D. B. Sullenger
H. L. Turner
R. E. Vallee
K. White
H. A. Woltermann
Records Center
Publications (1)
Library (15)